

# Slow Dynamics of the Cyclic Osmoregulated Periplasmic Glucan of *Ralstonia solanacearum* As Revealed by Heteronuclear Relaxation Studies

G. Lippens,\*<sup>†</sup> J.-M. Wieruszkeski,<sup>†</sup> D. Horvath,<sup>†</sup> P. Talaga,<sup>‡</sup> and J.-P. Bohin<sup>‡</sup>

Contribution from the CNRS URA 1309, Pasteur Institute of Lille, 1, rue du Professeur Calmette, 59000 Lille, France, and CNRS UMR 111, Université des Sciences et Technologies de Lille, 59655 Villeneuve d'Ascq Cedex, France

Received March 26, 1997. Revised Manuscript Received June 27, 1997<sup>⊗</sup>

**Abstract:** <sup>13</sup>C relaxation data obtained at different field strengths are reported for the osmoregulated periplasmic glucan (OPG) of *Ralstonia solanacearum*. Previous studies on this molecule showed that it is composed of 13 glucose units, linked all but one via  $\beta$ -(1–2) (Talaga et al. *J. Bacteriol.* **1996**, *178*, 2263–2271). The single  $\alpha$ -(1–6) linkage induces structural constraints to such an extent that all individual anomeric proton resonances could be distinguished, opening the possibility of a genuine structure determination of this molecule. The relaxation data in this report agree well with the dynamical data extracted from the off-resonance ROESY experiments (Lippens et al. *J. Am. Chem. Soc.* **1996**, *118*, 7019–7027), but indicate as well an important exchange contribution to the  $T_2$  relaxation times. This latter event was shown to result from a large-scale motion on the microsecond time scale, especially affecting the residues downstream of the  $\alpha$ -(1–6) linkage. Future atomic models of the compound will have to take into account the presence of conformational exchange.

## Introduction

Since the description of the cyclic all- $\beta$ -(1–2) osmoregulated periplasmic glucans (OPG) of the gram-negative bacteria of the *Rhizobiaceae*, there has been a considerable interest to determine the structural features of these molecules, as their physiological function is assumed to be closely related to their conformation.<sup>1</sup> Unfortunately, both the <sup>1</sup>H and <sup>13</sup>C NMR spectrum of these molecules are completely degenerate to that of one single glucose molecule. The homopolymeric nature and large size of these molecules, with a minimal<sup>2</sup> degree of polymerization (DP) of 17, and the degeneracy of the NMR spectra leave little hope of obtaining a model based on experimental constraints. Other techniques such as small-angle X-ray scattering, however, have shown some promise in alleviating the lack of experimental data.<sup>3</sup>

Recently, several OPG of different gram-negative bacteria were described that include one single  $\alpha$ -(1–6) linkage next to all  $\beta$ -(1–2) linkages.<sup>4</sup> This single  $\alpha$ -(1–6) linkage induces constraints to such an extent that all anomeric proton and carbon resonances appear as individual lines in a high-resolution NMR spectrum, and might therefore allow the former restrictions to be overcome. We have chosen the cyclic OPG of *Ralstonia*

*solanacearum* (previously *Burkholderia solanacearum*) as a working model because of its low degree of polymerization (DP13) and easy availability. Previous efforts to obtain structural parameters by NMR resulted in the precise measurement of the interglycosidic H1–H2' distances through the off-resonance ROESY method<sup>5</sup> and the heteronuclear <sup>3</sup>J coupling constants over the glycosidic linkage.<sup>6</sup> The former series of experiments involving the off-resonance ROESY technique also yielded values for the pairwise correlation times of the proton pair considered. These correlation times were fairly homogeneous over the different interglycosidic linkages, with a mean value of  $\tau_c = 0.9$  ns. However, these studies also indicated a caveat for a possible structural model, as an important line broadening of one anomeric proton resonance was observed. We therefore set out for a detailed study of the dynamics of the molecule.

A presently well-established approach to the investigation of dynamical properties in carbohydrates (and other biomolecules) is by means of heteronuclear relaxation measurements.<sup>7</sup> A “model-free” analysis of the relaxation rates has been proposed, decoupling the overall tumbling motion and the local motion where the extent and dynamics of the latter are characterized by an order parameter  $S^2$  and a local correlation time.<sup>8</sup> Moreover, in several studies, especially in proteins, it has been necessary to extend the parameter set to obtain consistency

\* To whom correspondence should be addressed.

<sup>†</sup> Pasteur Institute of Lille.

<sup>‡</sup> Université des Sciences et Technologies de Lille.

<sup>⊗</sup> Abstract published in *Advance ACS Abstracts*, December 15, 1997.

(1) (a) Palleschi, A.; Crescenzi, V. *Gazz. Chim. Ital.* **1985**, *115*, 243–245. (b) Serrano, G.; Franco-Rodriguez, G.; Gonzalez-Jimenez, I.; Tejero-Mateo, P.; Molina Molina, J.; Dobado, J. A.; Mégias, M.; Romero, M. *J. Mol. Struct.* **1993**, *301*, 211–226. (c) Poppe, L.; York, W. S.; van Halbeek, H. *J. Biomol. NMR* **1993**, *3*, 81–89. (d) André, I.; Mazeau, K.; Taravel, F. R.; Tvaroska, I. *Int. J. Biol. Macromol.* **1995**, *17*, 189–198. (e) André, I.; Mazeau, K.; Taravel, F. R.; Tvaroska, I. *New J. Chem.* **1995**, *19*, 331.

(2) York, W. S.; Thomson, J. U.; and Meyer, B. *Carbohydr. Res.* **1993**, *248*, 55–80.

(3) Mimura, M.; Kitamura, S.; Gotoh, S.; Takeo, K.; Urakawa, H.; Kajiwara, K. *Carbohydr. Res.* **1996**, *289*, 25–37.

(4) (a) Lippens G.; Talaga, P.; Wieruszkeski, J.-M.; Bohin, J.-P. In *Spectroscopy of Biological Molecules*; Merlin, J. C., Turrell, S., Huvenne, J.-P., Eds.; Kluwer Academic Publishers: Dordrecht, the Netherlands, 1995. (b) Talaga, P.; Stahl, B.; Wieruszkeski, J.-M.; Hillenkamp, F.; Tsuyumu, S.; Lippens, G.; Bohin, J.-P. *J. Bacteriol.* **1996**, *178*, 2263–2271. (c) York, W. S. *Carbohydr. Res.* **1995**, *278*, 205–225.

(5) Lippens, G.; Wieruszkeski, J.-M.; Talaga, P.; Bohin, J.-P.; Desvaux, H. *J. Am. Chem. Soc.* **1996**, *118*, 7227–7228.

(6) Lippens, G.; Wieruszkeski, J.-M.; Talaga, P.; Bohin, J.-P. *J. Biomol. NMR* **1996**, *8*, 311–318.

(7) For a review, see: Palmer, A. G., III; Williams, J.; McDermott, A. *J. Phys. Rev.* **1996**, *100*, 13293–13310 and references therein.

between the different relaxation data. An example is the ad hoc inclusion of an exchange term into the expression of the  $T_2$  relaxation rate,<sup>9</sup> or, recently, the anisotropy of the rotational diffusion as a supplementary parameter.<sup>10</sup>

In this report, we give the results of a complete heteronuclear relaxation study on the cyclic glucan of *R. solanacearum*. This study has allowed an experimental verification of the agreement between the correlation times stemming from the off-resonance ROESY experiment (that describe the motion of the proton-proton vector<sup>11</sup>) and the ones from the heteronuclear relaxation experiments, describing the motion of the  $^1\text{H}$ - $^{13}\text{C}$  vector. Secondly, the heteronuclear relaxation data yield very important information about the slow dynamics of the molecule, with exchange rates of the order of several microseconds. These data indicate that no unique conformation exists for the cyclic glucan, despite its unique spectral properties.

## Materials and Methods

The synthesis and purification of the native and labeled DP13 of *R. solanacearum* have been described previously.<sup>4</sup>

NMR experiments were performed at 301 K on a Bruker DMX 600 MHz spectrometer equipped with a triple-resonance probehead with a self-shielded  $z$  gradient. One  $T_2$  series was equally recorded on a Bruker DRX 300 MHz spectrometer. Samples contained 8 mg of native DP13 or 1.5 mg of  $^{13}\text{C}$ -enriched DP13 in 270  $\mu\text{L}$  of  $\text{D}_2\text{O}$  (Shigemi tube).

Pulse sequences used to measure the relaxation parameters started directly from carbon magnetization after NOE enhancement by preceding  $^1\text{H}$  decoupling,<sup>12</sup> or used a refocused INEPT transfer to accomplish magnetization transfer between proton and carbon magnetization.<sup>13</sup> Gradient pulses along the  $z$  axis were used to remove pulse imperfections and artifacts stemming from the imperfect refocusing of the antiphase components.<sup>14</sup> All experiments were invariably followed by a reverse INEPT sequence, in order to generate a heteronuclear correlation map. Low-power (2.6 kHz) GARP decoupling<sup>15</sup> was used during the acquisition period. The proton carrier was set to 4.2 ppm, whereas the  $^{13}\text{C}$  carrier was set to 82.5 ppm (with respect to TMSF).

For the 2D HSQC spectra, the 2.5 ppm  $^1\text{H}$  spectral window and 55 ppm  $^{13}\text{C}$  window were sampled with 1024 and, respectively, 128 complex points. The relaxation delay was set to 3 s, assuring complete relaxation of proton magnetization at the beginning of every scan. Eight scans were averaged for every increment. The spectra were processed as a  $2\text{K} \times 1\text{K}$  matrix after zero filling and multiplication by a Gaussian in  $\omega_2$  and a shifted sine function in  $\omega_1$ .

During the  $T_1$  inversion-recovery measurement, a low power GARP decoupling was applied to avoid relaxation in a coupled spin system<sup>16</sup> and cross correlation effects between dipolar and chemical shift anisotropy (csa) relaxation mechanisms.<sup>17</sup> Relaxation delays were chosen between 10  $\mu\text{s}$  and 3 s. The longitudinal relaxation  $T_1$  relaxation times were evaluated by a nonlinear least squares fit of the peak integrals

(8) (a) Halle, B.; Wennerström, H. *J. Chem. Phys.* **1981**, *75*, 1928–1943. (b) Lipari, G.; Szabo, A. *J. Am. Chem. Soc.* **1982**, *104*, 4546–4559. (c) Lipari, G.; Szabo, A. *J. Am. Chem. Soc.* **1982**, *104*, 4559–4557.

(9) Clore, G. M.; Driscoll, P. C.; Wingfield, P. T.; Gronenborn, A. M. *Biochemistry* **1990**, *29*, 7387–7401.

(10) Brüschweiler, R.; Liao, X.; Wright, P. *Science* **1995**, *268*, 886–889.

(11) (a) Desvaux, H.; Berthault, P.; Birlirakis, N. *Chem. Phys. Lett.* **1995**, *233*, 545. (b) Desvaux, H.; Berthault, P.; Birlirakis, N.; Goldman, M. *J. Magn. Res. A* **1994**, *108*, 219.

(12) Kay, L. E.; Torchia, D. A.; Bax, A. *Biochemistry* **1989**, *28*, 8972–8979.

(13) Morris, G. A.; Freeman, R. *J. Magn. Res.* **1979**, *101*, 760–762.

(14) (a) Kay, L. E.; Keifer, P.; Saarinen, T. *J. Am. Chem. Soc.* **1992**, *114*, 10663–10665. (b) Wider, G.; Wüthrich, K. *J. Magn. Res. B* **1993**, *102*, 239–241.

(15) Shaka, A. J.; Barker, P. B.; Freeman, R. *J. Magn. Res.* **1985**, *64*, 547–552.

(16) Dellwo, M. J.; Wand, A. J. *J. Magn. Res.* **1991**, *91*, 505–516.

(17) Boyd, J.; Hommel, U.; Campbell, I. D. *Chem. Phys. Lett.* **1990**, *175*, 477–482.

as implemented in the SNARF program (Frans van Hoesel, Groningen, the Netherlands).

Estimations of the  $T_2$  times were at first based on the intensity of the heteronuclear correlation peaks in a constant time experiment<sup>18</sup> with a constant time for  $^{13}\text{C}$ - $^{13}\text{C}$   $J$  evolution equal to 44 ms, corresponding to an average coupling constant of 45 Hz.

The  $T_2$  CPMG series was performed twice, once starting directly from carbon magnetization followed by a CPMG pulse train (see further in the main text), and once starting from proton magnetization and transfer to  $^{13}\text{C}$  magnetization via the refocused INEPT transfer. The two measurements gave independent values for the  $T_2$  relaxation times and allowed an estimation of the precision of these latter.

The initial CPMG measurements were performed with a 250  $\mu\text{s}$  delay separating the 26  $\mu\text{s}$   $^{13}\text{C}$   $\pi$  pulses. Care was taken to remove any cross correlation effects.<sup>19</sup> The duration of the CPMG pulse trains were chosen according to the results of a recent theoretical study where the Cramér-Rao theory was used to define an optimal sampling strategy.<sup>20</sup> The geometric mean of the extreme  $T_2$  times was estimated to  $T_{\text{GM}} = \sqrt{(T_{\text{min}}T_{\text{max}})} = 55$  ms, which leads to six equidistant CPMG times between 0 and 110 ms. As the fractional reliability of this sampling scheme drops near the extreme values of the range, we added a three-point series for the maximal  $T_2$  ( $T_2^{\text{max}} = 150$  ms), which practically consisted in adding a point at 1.6  $T_2^{\text{max}}$  or 240 ms, the other points already being included in the first series. For the inferior limit of 20 ms, we choose a four-point series constructed by adding two more points at 12 and 30 ms.

To investigate the contribution of chemical exchange to the  $T_2$  relaxation, several additional series with shorter  $\delta$  delays between the  $\pi$  pulses were recorded. Because short  $\delta$  values imply a large power delivery during the CPMG time with the possibility of sample heating, we added a CPMG time after the acquisition time, so as not to vary the average radio frequency power delivered in the different 2D experiments.<sup>21</sup> The maximal CPMG time in these series was set to 100 ms in the series of  $\delta$  values superior to 20  $\mu\text{s}$ , and to 62 ms in the series of  $\delta = 10$   $\mu\text{s}$ .

The NOE effect was measured as the difference in intensity of the direct correlation peak of the  $^{13}\text{C}$  magnetization starting with a 4-s delay during which a 1-kHz GARP proton decoupling was applied and a similar experiment where the proton decoupling was omitted.

The 1D versions of these experiments allowed extraction of some of the anomeric proton relaxation rates, as chemical shift dispersion is good in this region, and provided as such an independent measurement of the different relaxation rates. Error bars on measured relaxation rates were obtained by comparing the values obtained from a series of 1D measurements with those obtained from the full 2D relaxation series. As stated above, as the  $T_2$  relaxation times of the C2 carbon atoms proved to be crucial (see below), one 2D series of  $T_2$  measurement was repeated twice.

## Results and Discussion

### a. $T_1$ Relaxation Times and Heteronuclear NOE Values.

The  $T_1$  values of all carbon C1 resonances, when fitting the magnetization curves (Figure 1) measured on a  $^{13}\text{C}$ -labeled sample to a monoexponential<sup>22</sup> are fairly homogeneous, with values centered around 276 ms (Table 1). Error bars on the individual  $T_1$  times were estimated to  $\pm 3$  ms (see Materials and Methods). When measuring the  $T_1$  relaxation rates on a nonenriched sample, we systematically found longer values (data not shown). When checking for a possible influence of the sample concentration by comparing one-dimensional  $T_1$  data on a native and  $^{13}\text{C}$ -enriched sample at the same concentration,

(18) Vuister, G.; Bax, A. *J. Magn. Res.* **1992**, *98*, 428–435.

(19) Kay, L. E.; Nicholson, L. K.; Delaglio, F.; Bax, A.; Torchia, D. A. *J. Magn. Res.* **1992**, *97*, 359–375.

(20) Jones, J. A.; Hodgkinson, P.; Barker, A. L.; Hore, P. J. *J. Magn. Res. B* **1996**, *113*, 25–34.

(21) Wang, A. C.; Bax, A. *J. Biomol. NMR* **1993**, *3*, 715–720.

(22) Strictly speaking, this system behaves as a coupled two-spin system (see ref 16), but the carbon-carbon dipolar cross-relaxation is relatively small.

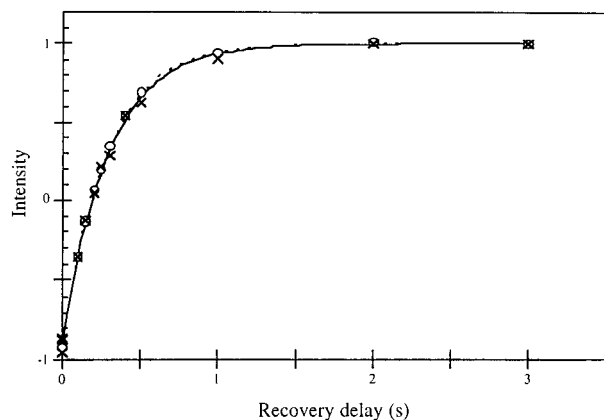


**Figure 1.**  $T_1$  recovery curves for the mC1 carbon resonance of the native (—x—) and  $^{13}\text{C}$ -enriched (—o—) DP13 of *R. solanacearum*. The least-squares fit gives a value of 293 ms for the former and 283 ms for the latter.

**Table 1.** (a)  $T_1$  and NOE Values for the C1 and C2 Carbons of the Cyclic OPG of *R. solanacearum*, As Measured on a  $^{13}\text{C}$ -Enriched Sample at 301 K and (b) for Other Selected Carbon Resonances<sup>a</sup>

a				
residue	$T_1$ (C1) (ms)	$T_1$ (C2) (ms)	NOE (C1) %	NOE (C2) %
a	269	257	35	33
f	283@	296	36@	42
i	274&	257	35&	34
j	274&	261	35&	33
d	281	262	34	26
l	280§	278	34§	29
b	268	284	34	36
e	274	281#	34	32°
k	280§	268	34§	31
c	274	280	32	32
h	269	281#	35	32°
g	283@	279	36@	34
m	281	273	35	38

b		
carbon	$T_1$ (C1) (ms)	NOE (%)
aC3	274	34
aC5	272	35
fC3	308	36
fC4	289	35
mC3	279	33
mC5	294	38

<sup>a</sup> Residues are labeled as in Figure 6. Overlapping resonances were grouped in pairs, indicated by special symbols. The average value is reported.

the difference consistently showed up. The average decrease of 14 ms for the C1 relaxation times upon  $^{13}\text{C}$  enrichment was therefore attributed to the contribution of the carbon-carbon dipolar interaction to the relaxation pathway, and is in good agreement with the 4.6% variation in the C $\alpha$   $T_1$  time when going from a singly toward a uniformly  $^{13}\text{C}$ -labeled alanine residue dissolved in perdeuterated glycerol at 40 °C where its correlation time  $\tau_c$  is equal to 1 ns.<sup>23</sup> The magnitude of the contribution of the  $^{13}\text{C}2$ - $^{13}\text{C}1$  homonuclear dipolar interaction being a monotonic function of correlation time, the observed difference is an independent estimate of a correlation time of the order of 1 ns.

The average  $T_1$  value of 290 ms found for the anomeric carbon resonances in the nonenriched sample agrees well with

(23) Yamazaki, T.; Muhandiram, R.; Kay, L. E. *J. Am. Chem. Soc.* **1994**, *116*, 8266–8278.

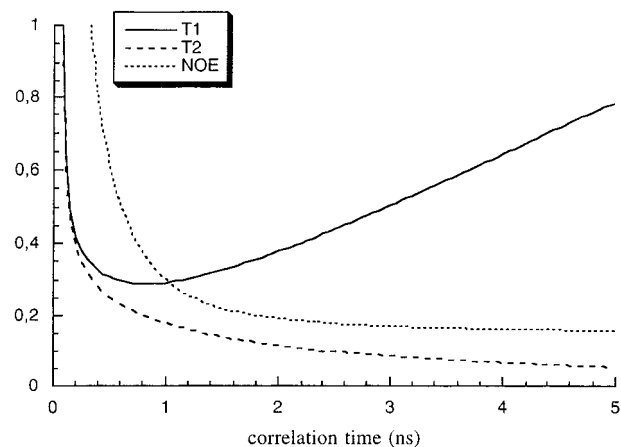


**Figure 2.** Contribution of the  $^1\text{H}$ - $^{13}\text{C}$  dipolar interaction to the  $^{13}\text{C}$   $T_1$  (—) and  $T_2$  (---) relaxation times (in seconds) calculated from the Lipari-Szabo model<sup>8</sup> using an overall tumbling time of 0.9 ns and an  $S^2$  value of 0.85. On the same plot, we have shown the theoretical NOE effect (···).

the theoretical value for a molecule that is tumbling with an overall correlation time of 0.9 ns and an order parameter  $S^2 = 0.85$  (Figure 2). The former value of the correlation time was also the average outcome of all pairwise correlation times as determined by the off-resonance ROESY experiment.<sup>5</sup> Despite the numerical agreement, one should keep in mind that both correlation times characterize different motional processes. The correlation time as determined by the off-resonance ROESY technique characterizes the time scale of the H1-H2' proton-proton vector movements,<sup>11</sup> whereas the correlation time obtained from the  $^{13}\text{C}$   $T_1$  values is mainly determined by the movement of the  $^1\text{H}$ - $^{13}\text{C}$  vector.<sup>24</sup> The good numerical agreement between the two correlation times indicates that the movements of the individual glucose units and the dynamics over the different glycosidic linkages are on a similar timescale.

The values for the C2  $T_1$  times show somewhat more of a spread, but are still well-conserved around a mean value of 271 ms. For the residues a and [i-j-d] flanking the  $\alpha$ -(1-6) linkage (for a numbering of the residues in the macrocycle, see Figure 6), a lower value of 260 ms was found, which could be explained by an increase to 0.95 of the  $S^2$  value. The only noticeably longer correlation time is observed for the f C2 residue. In this unit, the C2 carbon is not involved in a  $\beta$ -(1-2) linkage, and might hence experience a larger mobility than in the other residues. Similarly as for the anomeric carbon  $T_1$  values, an average increase of 18 ms was observed for the C2  $T_1$  values in the nonlabeled sample (data not shown). This increase is slightly larger than the one observed for the anomeric carbon  $T_1$  values, which can be explained by the difference in enrichment for both positions. The pairwise incorporation of  $^{13}\text{C}$  nuclei<sup>6</sup> and hence the occurrence of both  $^{13}\text{C}3$ - $^{13}\text{C}2$ - $^{13}\text{C}1$  and  $^{12}\text{C}3$ - $^{13}\text{C}2$ - $^{13}\text{C}1$  triplets leads to a complex multiexponential decay for the  $^{13}\text{C}2$  magnetization. Because all time constants are comparable, the values of a fit to a monoexponential curve are reported.

The good chemical dispersion around the  $\alpha$ -(1-6) linkage both at the  $^1\text{H}$  and  $^{13}\text{C}$  level allowed the determination of the  $T_1$  times of some other carbon nuclei. Therefore, we could verify whether the ring carbons in each ring are dynamically equivalent.<sup>25</sup> For both the a and m units, the values for all

(24) (a) Nirmala, N. R.; Wagner G. *J. Am. Chem. Soc.* **1988**, *110*, 7557–7558. (b) Peng, J.; Wagner, G. *J. Magn. Res.* **1992**, *98*, 308–332.

(25) Mäler, L.; Widmalm, G.; Kowalewski, J. *J. Biomol. NMR* **1996**, *1*, 1–7.

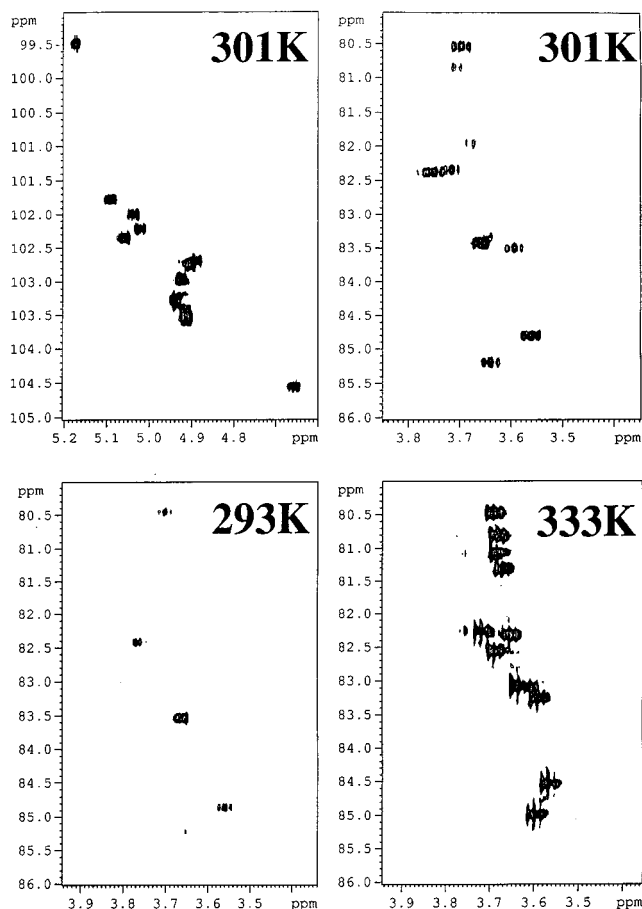


**Figure 3.** Selected regions of a constant-time HSQC spectrum: (a) H1–C1 region at 301 K; (b) H2–C2 region at 301 K; (c) H2–C2 region at 293 K; and (d) H2–C2 region at 333 K. The intensities were normalized with respect to the f H2–C2 correlation peak.

carbons in the hexacycle are very uniform (Table 1b), confirming that this unit moves as a rigid body. For the f unit, we see some more variation, which might point to an enhanced mobility for this residue implicated in the  $\alpha$ -(1–6) linkage.

The NOE values are also in good agreement with the theoretical value calculated for a  $\tau = 0.9$  ns correlation time (Figure 2). As we do not expect any influence of the carbon–carbon dipolar coupling, the measurements were only performed on the enriched sample. The theoretical expression for the NOE value contains spectral density terms in both the numerator and denominator. Therefore, this parameter shows no explicit dependency on the order parameter  $S^2$ , leaving us with a pure estimation of  $\tau_c$ . The average value of 34% is in excellent agreement with the previously determined value of 0.9 ns for  $\tau_c$ .

**b.  $T_2$  Relaxation Times.** On the basis of the same estimates of the correlation times  $\tau = 0.9$  ns and order parameter  $S^2 = 0.9$ , we expect  $T_2$  relaxation times of the order of 190 ms (Figure 2). A first indication of a discrepancy between these theoretical value and the experimental ones came from the observation of the constant-time HSQC on a  $^{13}\text{C}$ -enriched sample. The constant-time period for the evolution of the chemical shift was set to 44 ms, allowing a correct refocusing of the average  $^{13}\text{C}$ – $^{13}\text{C}$  one-bond  $J$  coupling constant.<sup>18</sup> In the spectrum of Figure 3a recorded at 301 K, all H1–C1 direct correlation peaks are visible, be it with a weaker intensity for the b C1 resonance. In the same spectrum, all H2–C2 correlation peaks are substantially weaker, and certain resonances such as the l unit almost disappear (Figure 3b).

More complete forms of the spectral density function  $J(\omega)$  that might potentially affect the  $T_2$  relaxation rates have been proposed. They include the presence of rapid internal motions<sup>8</sup> as well as an extended two time-scale model.<sup>26</sup> These more precise spectral density functions, however, affect the  $T_1$  and  $T_2$  relaxation rates in a similar manner, and cannot lead to the dramatic changes in observed  $T_2$  values (vide infra) while maintaining consistency with the observed  $T_1$  values. Anisotropic rotational diffusion<sup>10</sup> leads to a formally similar modification of the spectral density function, by introducing different correlation times according to the orientation of the C–H vector with respect to the axes of the diffusion tensor. However, because of the almost parallel orientation of the H1–C1 and H2–C2 internuclear vectors in the all-equatorial  $^4\text{C}_1$  chair conformation of the glucose rings, anisotropy would affect both C1 and C2 relaxation rates in a similar way. As the C1 carbons do not display the extremely fast  $T_2$  relaxation, this mechanism can be safely ruled out. Several other mechanisms such as chemical shift anisotropy (csa) and chemical exchange can add to the  $T_2$  relaxation and produce broader lines than expected on the basis of a purely dipolar relaxation mechanism.<sup>27</sup> It was previously shown that in a 25 residue peptide the csa contribution to the transverse relaxation for methionine  $\alpha$ -carbon nuclei with an estimated csa of 25 ppm can be neglected.<sup>28</sup> The complete  $^{13}\text{C}$  chemical shift tensors measured recently on single crystals of  $\beta$ -glucose and other glycosidic structures<sup>29</sup> indicate the same order of magnitude for the csa in the  $\beta$  glucose as found for the methine  $\alpha$ -carbon, and a value of 40 ppm was found for the C2 carbon in methyl- $\beta$ -glucose. Assuming an axially symmetric chemical shift tensor, the csa contribution to the  $T_2$  relaxation time is given by<sup>28</sup>

$$R_2^{\text{csa}} = \frac{(\Delta\delta)^2 \omega_c^2}{6} [4J(0) + 3J(\omega_c)] \quad (1)$$

By using a value of 40 ppm for  $\Delta\delta$  and  $\tau_c = 0.9$  ns, we find that the csa contribution is inferior to 1 Hz, and is thus not the main mechanism responsible for the additional broadening.

A strong indication that the additional line broadening is due to chemical exchange comes from the temperature dependence of the line broadening. For the anomeric proton resonance of unit b, we had previously found an increased broadening at lower temperatures.<sup>5</sup> At higher temperatures, the chemical exchange rate  $k_{\text{ex}}$  should increase, and hence contribute less to the exchange broadening. We tested this by recording constant-time HSQC spectra at different temperatures ranging from 20 to 60 °C. As can be seen in Figure 3c–d, the C2 resonances that are almost invisible at 20 °C gain considerably in intensity at the higher temperature, in agreement with the hypothesis of exchange broadening. The f C2 resonance, that is not involved in a linkage, provides a reference as it hardly changes in intensity upon increasing temperatures (data not shown).

More precise measurements of the  $T_2$  values were obtained with the 2D extension of the Carr–Purcell–Meiboom–Gill (CPMG) sequence<sup>30</sup> (Figure 4). The large distribution of expected  $T_2$  times (inferior to 40 ms for certain C2 resonances,

(26) Clore, G. M.; Szabo, A.; Bax, A.; Kay, L. E.; Driscoll, P. C.; Gronenborn, A. M. *J. Am. Chem. Soc.* **1990**, *112*, 4989–4991

(27) Abragam, A. *The Principles of Magnetic Resonance*; Clarendon Press: Oxford, UK, 1961.

(28) Palmer, A. G., III; Rance, M.; Wright, P. *J. Am. Chem. Soc.* **1991**, *113*, 4371–4380.

(29) Liu, F.; Phung, C. G.; Alderman, D. W.; Grant, D. M. *J. Am. Chem. Soc.* **1996**, *118*, 10629–10634.

(30) (a) Carr, H. Y.; Purcell, E. M. *Phys. Rev.* **1954**, *94*, 630–638. (b) Meiboom, S.; Gill, D. *Rev. Sci. Instrum.* **1958**, *29*, 688–691.

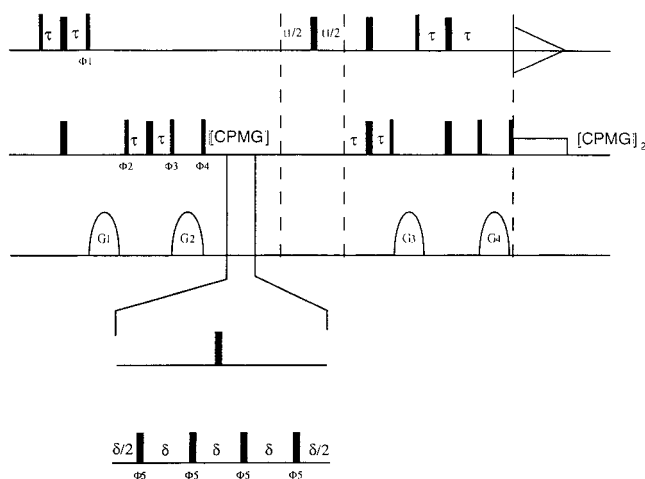


**Figure 4.** Pulse sequence used for the measurement of the  $T_2$  values. The CPMG block shown in insert was looped through the number of cycles needed to obtain the required CPMG time. After the acquisition period, the remaining CPMG loops were added such as to obtain the maximal CPMG time and ensure a constant (maximal) power dissipation during every point of the  $T_2$  series.<sup>21</sup> Pulse phase angles that are not indicated are equal to  $x$ . Other phases were  $\Phi_1 = y$ ,  $\Phi_2 = (x, -x)$ ,  $\Phi_3 = (y, -y)$ ,  $\Phi_4 = (x, -x)$ ,  $\Phi_5 = (y, -y)$ . The delay  $\tau$  was set to 1.52 ms. Pulsed gradients were applied as 1.3 ms sinusoidal pulses, with strengths of 30 Gauss/cm (G1), 25 Gauss/cm (G2), -18 Gauss/cm (G3), and -6 Gauss/cm (G4). Different series were recorded with the  $\delta$  delay in the CPMG train varying from 500  $\mu$ s to 10  $\mu$ s.

**Table 2.**  $T_2$  Values Measured on the Nonenriched OPG of *R. solanacearum* at 301 K and 150 MHz<sup>a</sup>

residue	$T_2$ (C1) (ms)	$T_2$ (C2) (ms)	$\Delta_{\text{ex}}$ C2 (Hz)
a	130	117	3
f	93 <sup>@</sup>	151	
i	81 <sup>#</sup>	64	11
j	81 <sup>#</sup>	53	14
d	107	33	25
l	92 <sup>§</sup>	19	54
b	47	27	33
e	89	18 <sup>#</sup>	50
k	92 <sup>§</sup>	45	15
c	81	21	38
h	124	18 <sup>#</sup>	50
g	93 <sup>@</sup>	29	28
m	136	24	35

<sup>a</sup> We used the CPMG sequence of Figure 4 with a delay  $\delta = 500$   $\mu$ s, and 11 CPMG times ranging from 1 ms to 240 ms (see main text). Overlapping resonances are grouped in pairs; see symbols. The average value is reported. Exchange contributions were calculated from  $(1/T_2^{\text{obs}} = 1/T_2^{\text{dip}} + \Delta_{\text{ex}})$  with a  $T_2^{\text{dip}} = 190$  ms.

based on the results of the constant-time HSQC experiment, and of the order of 150 ms for the a and m C1 resonance, based on preliminary 1D relaxation experiments) led to the delicate problem of choosing the CPMG times that should be used in the series of 2D experiments. The CPMG times were selected according to the results of a recent theoretical study where the Cramér–Rao theory was used to define an optimal sampling strategy<sup>20</sup> (see Materials and Methods). The results of the  $T_2$  measurements are summarized in Table 2. The series was repeated twice at 2-month intervals (see Materials and Methods), and the results proved reproducible to within  $\pm 2$  ms.

Whereas the values of all C1 resonances except for the b unit experience relatively little exchange broadening, the b C1 and even more all C2 resonances are dramatically broadened. With a purely dipolar  $T_2$  value of 190 ms based on the estimates of 0.9 ns for the correlation time and 0.85 for the order parameter  $S^2$ , the exchange contribution to the b C1 line width can be

**Table 3.**  $T_2$  Values Measured on the Nonenriched OPG of *R. solanacearum* at 301 K and 75 MHz<sup>a</sup>

residue	$T_2$ (C2) (ms)	$\Delta_{\text{ex}}$ C2 (Hz)	$\Delta_{\text{ex}}$ (14 T)/ $\Delta_{\text{ex}}$ (7 T)
a	ND	ND	ND
f	122 $\pm$ 5	0	
i	84 $\pm$ 7	4.4	3.2
j	84 $\pm$ 6	4.4	3.2
d	75 $\pm$ 6	5.8	4.3
l	59 $\pm$ 10	9.4	5.7
b	64 $\pm$ 6	8.1	4.1
e	ND	ND	ND
k	ND	ND	ND
c	ND	ND	ND
h	ND	ND	ND
g	73 $\pm$ 10	6.2	4.5
m	57 $\pm$ 7	10.0	3.5

<sup>a</sup> Exchange contributions were calculated from  $(1/T_2^{\text{obs}} = 1/T_2^{\text{dip}} + \Delta_{\text{ex}})$  with  $T_2^{\text{dip}} = 133$  ms.

estimated to 14 Hz, whereas for certain C2 resonances, it obtains values as large as 54 Hz (Table 2). Alternatively, we could consider the fC2  $T_2$  relaxation time as the basis for the nonexchange broadened  $T_2$  value, but this leads to no major differences for the exchange term.

**Field Dependence of the  $T_2$  Relaxation Times.** In the constant-time HSQC experiment, only one 180° <sup>13</sup>C pulse is applied during the delay of 44 ms; therefore no refocusing of the chemical exchange can happen (vide infra), and the exchange contribution is given by<sup>32</sup>

$$\Delta_{\text{ex}} = \frac{1}{8} \frac{\Omega_{\text{ex}}^2}{k_{\text{ex}}} \quad (2)$$

The quadratic dependence on  $\Omega_{\text{ex}}$ , the chemical shift separation (in radial units) of the different chemical species, emphasizes that physically an exchange process is similar to the molecular self-diffusion process, here in one dimension.<sup>33</sup> Furthermore, the analytical dependence of the exchange contribution on the quadratic difference in chemical shift for the coexisting conformations suggests a straightforward way of verifying the nature of the broadening mechanism. We recorded at 301 K a series of  $T_2$  experiments at the lower field of 7.1 T (or 75 MHz for <sup>13</sup>C). The disadvantage of the lower field strength was the decrease in sensitivity and the increased spectral overlap, leading to considerably higher uncertainties in the  $T_2$  values. Still, the good separation of the H2–C2 correlation peaks allowed us to extract a certain number of them (Table 3). If again we estimate the dipolar contribution to the  $T_2$  relaxation time on the basis of a correlation time  $\tau_c = 0.9$  ns and an average order parameter  $S^2 = 0.85$ , we obtain a value of 133 ms. Subtracting this dipolar contribution from the observed relaxation rates, we obtain the exchange contribution at 75 MHz (Table 3), and can evaluate the ratio of the exchange contributions at 14.1 and 7.1 T. By taking into account the large uncertainties on the  $T_2$  values at the lower field of 7.1 T, the obtained ratios are reasonably close to the theoretical value of 4 as expected from eq 2.

**Characterization of the Time Scales of the Exchange Process.** The quadratic expression of the exchange contribution to the  $T_2$  relaxation is valid when the  $T_2$  is evaluated as the characteristic decay time of the freely precessing signal. Most measurements of  $T_2$  relaxation rates do not use the line width

(31) Bloom, M.; Reeves, L. W.; Wells, E. J. *J. Chem. Phys.* **1965**, *42*, 1615–1624.

(32) Kaplan, J. I. In *Encyclopedia in Nuclear Magnetic Resonance*; Grant; Harris, Eds.; 1995; Vol. 2, p 1252.

(33) Woessner, D. E. *J. Chem. Phys.* **1961**, *35*, 41.

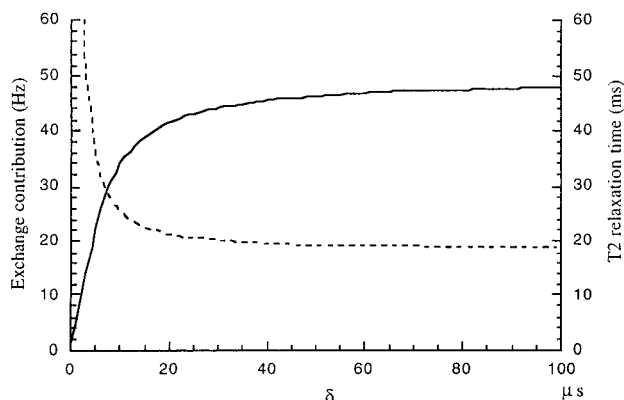


**Figure 5.** Exchange contribution (—) and resulting  $T_2$  relaxation time (---) as a function of the  $\delta$  delay used in the CPMG period (Figure 3). The curves were calculated according to eq 3 with values of  $\Omega_{\text{ex}} = 2\pi \times 1200$  Hz,  $k_{\text{ex}} = (7 \mu\text{s})^{-1}$ , and  $T_2^{\text{dip}} = 133$  ms.

of the freely precessing signal, but incorporate a CPMG<sup>30</sup> pulse train in a heteronuclear correlated spectrum, in order to profit simultaneously from the enhanced sensitivity of the proton detection and the good spread in heteronuclear chemical shift. It has been recognized early on that both definitions of  $T_2$  are not necessarily equivalent. In the presence of chemical exchange, the exchange contribution to the  $T_2$  relaxation times depends on the delay  $\delta$  used between the  $180^\circ$  pulses in the CPMG pulse train of Figure 4. In the case of fast exchange, i.e.,  $k_{\text{ex}} > \Omega_{\text{ex}}$ , the exchange contribution  $\Delta_{\text{ex}}$  to the  $T_2$  relaxation time is<sup>31</sup>

$$\Delta_{\text{ex}} = \frac{1}{4} \left[ k_{\text{ex}} - \frac{1}{2\delta} \sinh^{-1}(\delta k_{\text{ex}} \sinh(2u)/u) \right] \quad (3)$$

with

$$u = \delta \sqrt{k_{\text{ex}}^2 - \Omega_{\text{ex}}^2}$$

When the duration of  $\delta$  is short compared to the time constant for exchange, the effects of chemical exchange are continuously refocused and hence attenuated. In the limit of vanishingly small  $\delta$ ,  $\Delta_{\text{ex}}$  will tend to zero, but for values of  $\delta$  that are nonzero but still appreciably smaller than  $(k_{\text{ex}})^{-1}$ , an approximately linear relationship results (see Figure 5). However, various experimental factors might interfere with this theoretical prediction. Decreasing  $\delta$  corresponds to an increased power delivery, leading to possible artifacts in the CPMG sequence such as (i) hardware imperfections, both as pulse imperfections or drops in sustained power levels, (ii) temperature rise leading to an increased exchange rate and decreased  $\tau_c$  value—both factors will lead to a decrease in  $T_2$  relaxation rate, (iii) changes in possible antiphase components, where the relaxation of these latter differs from the desired in-phase magnetization,<sup>34</sup> and (iv) changes in possible systematic off-resonance effects.<sup>35</sup>

As a first guess for the chemical shift difference of the carbon nuclei in the multiple chemical environments, we can take the total spread of all C1 (or C2) resonances found in the molecule. For the bC1 resonance, assuming a spread of 2 ppm, which covers all C1 resonances except for the a and m units, a 15-Hz exchange contribution leads to an estimate for  $k_{\text{ex}} = (33 \mu\text{s})^{-1}$ , whereas the observed  $\Delta_{\text{ex}} = 50$  Hz for the C2 resonances

**Table 4.**  $T_2$  Values of the C2 Resonances Measured on the Nonenriched OPG of *R. solanacearum* at 301 K<sup>a</sup>

residue	$T_2$ ( $\delta = 100 \mu\text{s}$ )	$T_2$ ( $\delta = 50 \mu\text{s}$ )	$T_2$ ( $\delta = 20 \mu\text{s}$ )	$T_2$ ( $\delta = 10 \mu\text{s}$ )
i	63	58	65	ND
j	56	55	56	ND
d	33	37	32	36
l	19	20	24	25
b	31	31	34	36
e	21 <sup>#</sup>	22 <sup>#</sup>	21 <sup>#</sup>	24 <sup>#</sup>
k	42	43	45	46
c	22	23	25	27
h	21 <sup>#</sup>	22 <sup>#</sup>	21 <sup>#</sup>	24 <sup>#</sup>
g	33	38	40	38
m	27	26	27	27

<sup>a</sup> The CPMG sequence of Figure 4 with different  $\delta$  delays was used. Because only CPMG times up to 62 ms were taken for the series with  $\delta = 10 \mu\text{s}$ , the fit for the longer  $T_2$  values could not be determined reliable.

combined with a total spread of 5 ppm leads to an estimated value of  $k_{\text{ex}} = (18 \mu\text{s})^{-1}$ .

The theoretical expression of eq 3 and its graphical representation as shown in Figure 5 indicate how to experimentally narrow down the range of possible  $k_{\text{ex}}$  values. Indeed, reducing the  $\delta$  period between the  $\pi$  pulses in the CPMG train to smaller values should reduce the exchange contribution, at least if the values of  $\tau_{\text{ex}} = 1/k_{\text{ex}}$  and  $\delta$  become comparable.<sup>36</sup> Recently, this approach was used to measure the <sup>15</sup>N main-chain dynamics in four forms of staphylococcal nuclease with different stabilities to unfolding.<sup>37</sup> The results of our  $T_2$  experiments using different  $\delta$  delays in the CPMG relaxation delay are summarized in Table 4.

Whereas the results at the shortest  $\delta$  delay ( $\delta = 10 \mu\text{s}$ ) are the most instructive, they are also hampered by the largest experimental difficulties. Indeed, we observed a significant drop in the lock level after the CPMG period, most probably due to a rise in temperature caused by the increased power dissipation delivered by the train of <sup>13</sup>C  $\pi$  pulses separated only by a short interpulse delay  $\delta$  of  $10 \mu\text{s}$ . Although this might influence the  $T_2$  measurements as stated above, we do observe a systematic increase in  $T_2$  relaxation time upon going to shorter  $\delta$  values. This effect is the most pronounced for the units with the largest exchange contribution to the C2  $T_2$  relaxation, i.e., units l and c. Fitting the parameters  $\Omega_{\text{ex}}$  and  $k_{\text{ex}}$  in order to reproduce the  $T_2$  values of both C2 resonances, we obtain a reasonable agreement for  $\Omega_{\text{ex}} = 2\pi \times 1200$  Hz and  $k_{\text{ex}} = (7 \mu\text{s})^{-1}$  (Figure 5). The main surprise of the fit is the very large chemical shift difference that is predicted for the coexisting species. The chemical shift range of the C2 resonances is limited to about 5 ppm or 750 Hz. Of course, the observed chemical shift value is the average between the chemical shift values in the two (or more) positions, leading to a possible chemical shift range superior than the one observed. A concrete example of this is formed by the l C2 resonance. The observed chemical shift value of 79.96 ppm at the low-field edge of the C2 resonances must be the average over at least two values. If we take for one value the opposing edge of the C2 resonances, i.e. 85.17 ppm (as observed for the dC2 resonance, see Figure 3b), the other chemical shift value must be at 75 ppm, yielding a value of  $2\pi \times 1500$  Hz for  $\Omega_{\text{ex}}$ . Whereas these extreme values fall largely outside the usual chemical shift range as observed for C2 resonances of  $\beta$ -substituted glucose residues, it should be

(34) Peng, J. W.; Thanabal, V.; Wagner, G. *J. Magn. Res.* **1991**, *94*, 82–93.

(35) Ross, A.; Czisch, M.; King, G. C. *J. Magn. Res.* **1997**, *124*, 355–365.

(36) Orekhov, V. Y.; Pervushin, K. V.; Arseniev, A. S. *Eur. J. Biochem.* **1994**, *219*, 887–896.

(37) Alexandrescu, A. T.; Jahnke, W.; Wiltscbeck, R.; Blommers, M. J. *J. Mol. Biol.* **1996**, *260*, 570–587.

**Table 5.**  $T_2$  Values of the C2 Resonances Measured on the Nonenriched Sample of *R. solanacearum* at 288 K and 150 MHz<sup>a</sup>

residue	$T_2$ ( $\delta = 500 \mu\text{s}$ )	$\Delta\text{ex}$	$T_2$ ( $\delta = 10 \mu\text{s}$ )	$\Delta\text{ex}$
bC1	19	40	39.8	18.5
jC2	22	38	35	22
dC2	15	57	25	33
kC2	20	44	30	26.2
gC2	14	64	32	24.1
mC2	13.0	70	24	35

<sup>a</sup> The CPMG sequence of Figure 4 with different  $\delta$  delays was used. Only CPMG times up to 62 ms were taken for the series with  $\delta = 10 \mu\text{s}$ , therefore the fit for the longer  $T_2$  values could not be determined reliable. Exchange contributions were calculated from  $(1/T_2^{\text{obs}} = 1/T_2^{\text{dip}} + \Delta\text{ex})$  with a  $T_2^{\text{dip}} = 150 \text{ ms}$ .

noted that variations in chemical shift up to 12 ppm have previously been observed for carbon atoms flanking a glycosidic linkage.<sup>38</sup> For the DP13 molecule of *R. solanacearum*, the specific structural constraints and hence peculiar positions in the Ramachandran plot might be at the basis of such divergent chemical shift values.

As many experimental errors are possibly associated with decreasing the  $\delta$  delay in the CPMG pulse train, we developed the following more qualitative estimate for both the exchange rate and the chemical shift differences between the different conformations. Even for the shortest  $\delta$  delay between the  $\pi$  pulses, all  $T_2$  relaxation rates remain substantially faster than the expected dipolar  $T_2$  value. The possible artifacts upon increasing power delivery will all tend to decrease the relaxation rate; therefore, we can conclude that for  $\delta = 10 \mu\text{s}$ , chemical exchange is still fully active in the observed line broadening. Our initial estimate for the exchange rate,  $k_{\text{ex}} = (20 \mu\text{s})^{-1}$ , is hence too low, and  $k_{\text{ex}} = (10 \mu\text{s})^{-1}$  is a reasonable lower limit on its value. Secondly, the still acceptable values of the chemical shift differences inferred from the fit allow us to establish with some confidence an upper limit. Indeed, an increase of the exchange rate by a factor of 4 to a value of  $(2 \mu\text{s})^{-1}$  implies a 2-fold increase of  $\Omega_{\text{ex}}$  in order to maintain the same exchange contribution, which is very improbable in view of the range of chemical shift values previously observed.<sup>38</sup> Both arguments validate qualitatively the value for  $k_{\text{ex}}$  obtained from our fitting procedure, despite the limited variation in  $T_2$  as function of  $\delta$ .

**Exchange Data at a Lower Temperatures.** The variations observed for the  $T_2$  relaxation times at 301 K upon varying the  $\delta$  delay in the CPMG pulse train are limited (Table 3). Further decreasing this value would lead to an excessive power delivery and cannot realistically be performed with our current hardware. We therefore decided to work at a lower temperature, thereby decreasing the exchange rate. The values at 288 K are shown in Table 5. Some C2 carbons corresponding to the shortest  $T_2$  relaxation time at 301 K disappear completely, probably due to  $T_2$  relaxation during the INEPT periods in the refocused HSQC of Figure 3. However, for the still visible resonances, the variations in  $T_2$  relaxation rates using a CPMG pulse train with an interpulse delay of 500 or 10  $\mu\text{s}$  are important at this lower temperature, in agreement with a decrease in exchange rate to below  $(10 \mu\text{s})^{-1}$ . Assuming a purely dipolar  $T_2$  relaxation time of 150 ms, the exchange contributions derived from the  $T_2$  relaxation times at 288 K obtained with a  $\delta$  value of 500  $\mu\text{s}$  are on the average a factor of 2.4 longer than the corresponding values at 301 K. In the hypothesis of negligible changes in occupancy and chemical shift values of the different conformations,

**Table 6.** The Chemical Shift Values of the C2 Carbons in the Individual Conformations<sup>a</sup>

residue	$\omega$ (average)	$\omega$ (low)	$\omega$ (high)
a	83.4	82.4	84.4
f	74.9	74.9	74.9
i	82.4	84.0	80.8
j	84.8	86.9	82.7
d	85.2	88.0	82.4
l	80.0	84.2	75.8
b	82.4	85.7	79.1
e	81.0	85.0	77.0
k	80.6	82.8	78.4
c	83.4	86.9	79.9
h	81.0	85.0	77.0
g	83.5	86.5	80.5
m	82.0	85.4	78.6

<sup>a</sup> The average chemical shifts were those reported for the DP13 molecule at 301 K (ref 4), and the chemical shift difference between the two forms involved was calculated as  $\omega_{\text{av}} \pm \Omega_{\text{ex}}/2$ , using eq 2 and the exchange contributions of Table 2.

mational states, this implies that the chemical exchange is slowed down by the same factor, i.e.,  $k_{\text{ex}} \approx (17 \mu\text{s})^{-1}$ .

The above-derived temperature dependence allows a rough estimate for the experimental conditions that should be obeyed for NMR separation of the different conformations. The exchange-broadened peak will split into two separate peaks when the condition  $\Omega_{\text{ex}}/k_{\text{ex}} > 4$  is fulfilled.<sup>32</sup> For an estimated maximal value of  $2\pi \times 1500 \text{ Hz}$  for  $\Omega_{\text{ex}}$ , this condition implies that the exchange should slow down to  $(500 \mu\text{s})^{-1}$ . By assuming a temperature-independent activation barrier, i.e., every decrement of 13 K slows down the interconversion by a constant factor of 2.4, splitting of the lines requires NMR spectra at 236 K. Previous measurements of disaccharides in an undercooled aqueous solution aimed at the observation of exchangeable hydroxyl protons involved in hydrogen bonds have demonstrated the possibility to attain temperatures as low as 257 K.<sup>39</sup> In similar experiments with the DP13 of *R. solanacearum*, we have reached 265.0 K in a capillary tube (spectra not shown), but the limit of 236 K is obviously not attainable without the addition of cosolvents. This possibility is currently under investigation in our laboratory.

**Structural Aspects of the Chemical Exchange Data.** The above described results indicate unambiguously that the oligosaccharide passes through different conformations that are in dynamic exchange on the microsecond time scale. One major problem of any NMR study on a system that shows rapid chemical exchange is the average nature of all obtained structural parameters. A very illustrative example is formed by the cyclic decapeptide antanamide, for which the available NOE and  $J$  coupling data could not be satisfied by one single conformation.<sup>40</sup> The simplest model compatible with all NMR parameters required two different conformations. Another extreme example of the average nature of the NMR parameters is formed by the all  $\beta$ -(1-2) cyclic glucans of the *Rhizobiaceae*. Both the chemical shift values and the  $^3J$  coupling constants measured over the glycosidic linkage reflect an average behavior over both the individual monomers and over the different conformations adopted by the macrocycle over time.<sup>1</sup>

Our initial hope when starting the structural studies on the OPG of *R. solanacearum* was that the single  $\alpha$ -(1-6) linkage would induce structural constraints to such an extent that both mechanisms of averaging would be greatly reduced. Whereas the first averaging evidently has disappeared—we observe all

(39) Poppe, L.; van Halbeek, H. *Nat. Struct. Biol.* **1994**, *1*, 215–216.

(40) Kessler, H.; Griesinger, C.; Lautz, J.; Müller, A.; van Gunsteren, W. F.; Berendsen, H. J. C. *J. Am. Chem. Soc.* **1988**, *110*, 3393–3396.

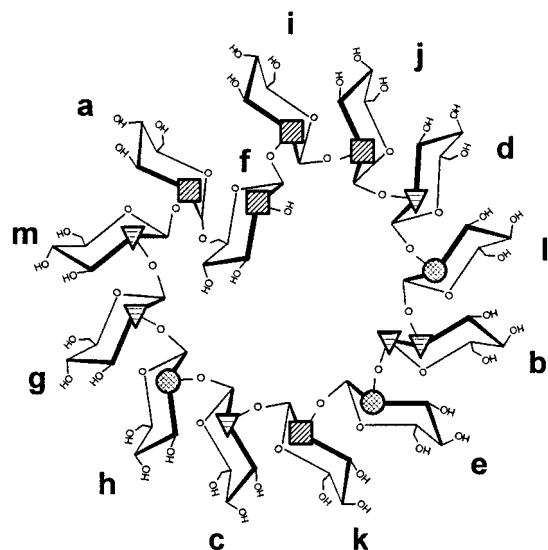


**Figure 6.** The macrocycle of the DP13 OPG of *R. solanacearum*. The symbols on the C2 carbons graphically represent the exchange contribution to the  $T_2$  relaxation of the C2 nucleus. Circles represent exchange contributions  $\Delta_{\text{ex}} > 50$  Hz, triangles correspond to  $\Delta_{\text{ex}} = 20\text{--}30$  Hz, and squares correspond to  $\Delta_{\text{ex}} < 10$  Hz. All C1 carbons except for the bC1 have values of  $\Delta_{\text{ex}}$  inferior to 10 Hz.

anomeric protons resonances individually—the above-described relaxation data show that our structural data still result from an average over two or more conformations.

It is illustrative to map the exchange contribution on the macrocycle (Figure 6). With the exception of the b unit, only the C2 carbon  $T_2$  values are appreciably affected by the chemical exchange, implying the most important variation for the  $\Psi$  angle between the different conformations. We further observe that chemical exchange is not uniformly distributed over the macrocycle, as the residues around the  $\alpha$ -(1–6) linkage are relatively little affected, whereas the main exchange phenomenon takes place around the b unit, diametrically opposed to the a–f linkage. For the latter b residue, both C1 carbon and C2 carbon are considerably broadened. In the case of the DP16 molecule of *Xanthomonas campestris*, York presented recently a structural model, and proposed a topological reversal point between the two helical domains to occur at the level of the flexible  $\alpha$ -(1–6) linkage and at the residue where a frameshift in the alternating chemical shift pattern was observed.<sup>4</sup> Our current hypothesis is that this point of asymmetry in the DP13 molecule of *R. solanacearum* occurs at the level of the b residue, but not in a static fashion, i.e., that the point hops between both linkages preceding or following this b residue.

When we consider the simplest model where only two conformations are present in equal proportions, the relaxation data allow us to calculate the chemical shift values of every C2 carbon resonance in one or the other conformation. On the basis of the previously obtained averaged chemical shift values<sup>4</sup> and

the values for the exchange contribution (Table 2), the chemical shift values of the C2 carbons in the individual conformations can be obtained as  $\omega_{\text{av}} \pm \Omega_{\text{ex}}/2$  (Table 6), providing as such unique information about the C2 nuclei in one or the other conformation.

In the  $^{13}\text{C}$  NMR spectra of oligo- and polysaccharides, the chemical shifts of the carbon atoms on either side of the glycosidic linkage have been found to vary over a range of up to 12 ppm, depending on the conformation of the linkage.<sup>38</sup> Excluding the f C2 carbon that is not implicated in a linkage, we find here variations of 14 ppm for the C2 resonance positions, indicating a large conformational variety. A similar phenomenon is observed at the level of the b C1 resonance, where the exchange contribution to  $T_2$  of 16 Hz leads to an estimated 4 ppm between the extreme chemical shift values, close to the entire range of C1 chemical shift values observed. It should be mentioned at this point that we cannot yet distinguish whether for a given C2 nuclei the high or low chemical shift value corresponds to the one or another conformation, but the combination of these data with the previously determined short distances and  $^3J$  coupling constants<sup>5,6</sup> will probably allow the alleviation this ambiguity.

Anomeric and other related effects have been used to establish a relationship between chemical shift and glycosidic conformation based on the anomeric and related effects.<sup>38</sup> The possibility of obtaining chemical shift values by quantum calculations, as has been pioneered by Oldfield et al. for proteins,<sup>41</sup> might be feasible on the smallest unit of the DP13 molecule, i.e., a disaccharide of two glucose units linked in  $\beta$ -(1–2). Chemical shift calculations over the whole Ramachandran plot for the carbons flanking the glycosidic bond can be combined with the chemical shift values derived for the C2 carbons in the individual conformations. The potential of chemical shift calculations therefore provides a new challenge in establishing a more accurate conformational model for the cyclic osmoregulated periplasmic glucan of *R. solanacearum* taking into account the chemical exchange.

**Acknowledgment.** We thank Professor A. Palmer (Columbia University, NY) and Dr. H. Desvaux (CEA, Paris, France) for fruitful discussions, and A. Bohin for precious help with the sample preparation. The 600-MHz facility used in this study was funded by the European Community (FEDER), the Région Nord–Pas de Calais (France), the CNRS and the Institut Pasteur de Lille. Part of this work was performed as a collaborative effort of the Laboratoire Européen Associé “Analyse structure-fonction des biomolécules” (CNRS, France–FNRS, Belgium) and of the Groupement Scientifique RMN Nord–Pas de Calais (France).

JA970960U

(41) Oldfield, E. *J. Biomol. NMR* **1995**, *5*, 217–225.